Electronic Supporting Information

Microcapsule Buckling Triggered by Compression-Induced Interfacial Chase Change

Andrew R Salmon,[1] Richard M Parker,[1] Alexander S Groombridge,[1] Armando Maestro,[1] Roger J Coulston,[1] Jonas Hegemann,[2] Jan Kierfeld,[2] Oren A Scherman,[1] Chris Abell[1] *

[1] University of Cambridge, Lensfield Road, Cambridge (UK) CB2 1EW

[2] TU Dortmund University, Physics Department, Otto-Hahn-Str 4, Dortmund (DE) 44221

* E-mail: ca26@cam.ac.uk

Derivation of Equation 6.

From the definition of the Poisson ratio the proportional change in film volume, $\Delta V_{film}/ V_{film,0}$, is given by:

$$\frac{\Delta V_{film}}{V_{film,0}} = \left(1 + \frac{\Delta L_{film}}{L_{film,0}}\right)^{1-2\nu}$$

where $\Delta L_{film}/L_{film,0}$ is a 1-dimensional film compression (or expansion). For an isotropic 2-dimensional (area) compression the volume change is:

$$\frac{\Delta V_{film}}{V_{film,0}} = \left(1 + \frac{\Delta L_{film}}{L_{film,0}}\right)^{2-4\nu}$$

Here, the compression corresponds to the area shrinkage of the droplets as:

$$\Delta L_{film} = \sqrt{4\pi R^2} - \sqrt{4\pi R_0^2}$$

And:

$$L_{film,0} = \sqrt{4\pi R_0^2}$$

The volume change relates to the film density by:

$$\frac{\Delta V_{film}}{V_{film,0}} = \frac{\rho_{film,0}}{\rho_{film}} - 1$$

Substituting in and simplifying, it is found that:

$$\rho_{film} = \rho_{film,0}\left(\frac{R_0}{R}\right)^{2-4\nu}$$

Which is Equation 6 in the main text

Size scaling with other polymer systems

Throughout this work the interfacial films are formed by cross-linking PVA-stil (Figure 1b) via homoternary host-guest complexes. It is important to confirm that the general phenomenology shown here also applies to other polymer systems. Figure S1 shows the scaling of the buckling diameter with material mass, as in Figure 2b, but instead for the cross-linked heteroternary PVA-mv/ PVA-stil polymer system that has previously been reported.[1] The same scaling rule applies which indicates that the fundamental mechanism is the same in both cases. The microcapsules with the heteroternary system are smaller for the same material mass, which may be a result of the polymer systems having different gelling properties.

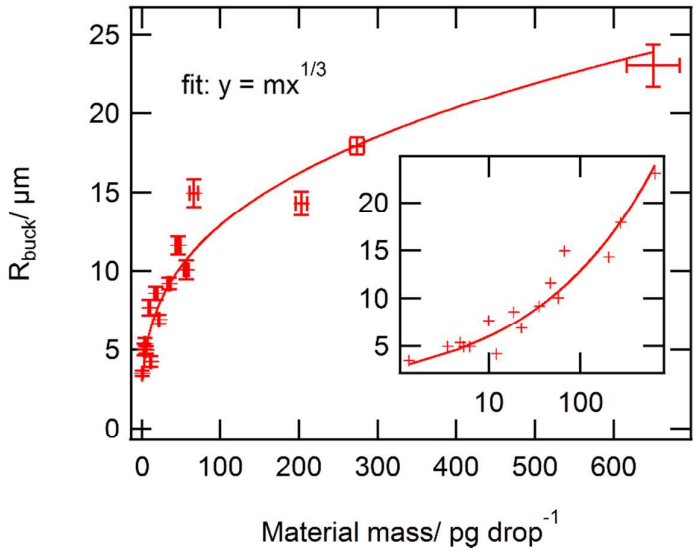

Figure S1. Buckling radius as a function of material mass per droplet, as in Figure 2a in the main text, but instead with (PVA-mv·PVA-stil)⊂CB[8] as the cross-linked interfacial polymer. Inset is the same on a logarithmic scale. The behavior of this polymer system is distinct, with a smaller buckling radius for the same material mass, but it follows the same scaling relationship indicative of a constant ratio $\left(\frac{T}{R}\right)_{buck}$.

Equilibrium calculations

Given that the cross-linking of the polymer chains is via a supramolecular ternary complex, it is natural to ask what role the equilibrium dynamics could play in the buckling transition.

The homoternary equilibrium constant $K_{a,homo}$ is defined as:

$$K_{a,homo} = \frac{[\mathrm{HGG}]}{[\mathrm{H}][\mathrm{G}]^2}$$

where [HGG], [H], and [G] are the equilibrium concentrations of host-guest complex, the host, and the guest respectively. In our system the polymers are localized to the droplet interface and as a result their local concentrations are greater than if they were evenly distributed through the droplet. This can be accounted for by considering the volumes accessible to each component:[2]

$$K_{a,homo} = \frac{[\mathrm{HGG}]}{[\mathrm{H}][\mathrm{G}]^2} = \frac{\left(\frac{n_{\mathrm{HGG}}}{V_{\mathrm{HGG}}}\right)}{\left(\frac{n_{\mathrm{H}}}{V_{\mathrm{H}}}\right)\left(\frac{n_{\mathrm{G}}}{V_{\mathrm{G}}}\right)^2}$$

where n_i is the number of moles in the volume V_i for each component i. It is convenient to define in terms of the concentration factor, $f_{conc,i}$:

$$f_{conc,i} = \frac{V_{drop}}{V_i}$$

where V_{drop} is the volume of the droplet.

Starting from initial concentrations of host, $\frac{n_{\mathrm{H}_0}}{V_{\mathrm{H}}}$, and guest, $\frac{n_{\mathrm{G}_0}}{V_{\mathrm{G}}}$, the equilibrium condition will be met where:

$$K_{a,homo} = \frac{\left(\frac{n_{\mathrm{HGG}}}{V_{\mathrm{HGG}}}\right)}{\left(\frac{n_{\mathrm{H}_0} - n_{\mathrm{HGG}}}{V_{\mathrm{H}}}\right)\left(\frac{n_{\mathrm{G}_0} - 2n_{\mathrm{HGG}}}{V_{\mathrm{G}}}\right)^2}$$

Rearranging to:

$$K_{a,homo}\frac{V_{\mathrm{HGG}}}{V_{\mathrm{H}}V_{\mathrm{G}}^2}\left(n_{\mathrm{H}_0} - n_{\mathrm{HGG}}\right)\left(n_{\mathrm{G}_0} - 2n_{\mathrm{HGG}}\right)^2 - n_{\mathrm{HGG}} = 0$$

which can be solved graphically by plotting the left hand side of the equation with a range of n_{HGG} and finding the axis intercept. This was done automatically in custom software, written in Igor Pro.

We can estimate that the concentration factor (f_{conc}) is at least ~50 by considering the interfacial layer to be initially at most 200 nm thick on a 30 μm radius droplet. This is justified from our hanging droplet measurements (Figure 3) where a 324 nm wall thickness was measured, as well as by AFM measurements. This estimate is likely very conservative as smaller radius capsules have thinner walls, and the hanging droplet measurement shows the wall thickness after compressive thickening. Consequently, a concentration factor of 50 is likely an underestimate.

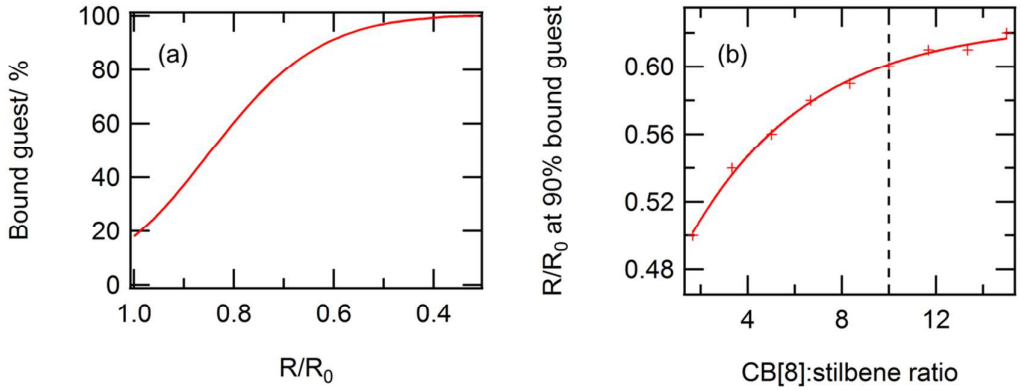

Figure S2. (a) Theoretical proportion of bound guest as a function of the droplet shrinkage ratio. As the droplet evaporates and its size decreases the concentration of the capsule components increases. This shifts the equilibrium towards bound guests. (b) Droplet shrinkage ratio at 90% bound guest as a function of the CB[8]:stilbene ratio; $f_{conc} = 50$, $K_a = 10^5$ M^{-2}

Equilibrium dynamics can plausibly play a role in capsule formation for the relatively weak-binding ternary host-guest complex considered here. During droplet evaporation the concentration of the capsule components increases and the equilibrium shifts towards bound guests (Figure S2a). In principle a buckling transition could be triggered by reaching an equilibrium-dependent cross-linking density. We believe that this mechanism contributes to the behavior observed in Figure 2b. With relatively low CB[8] concentrations the equilibrium binding is a factor that influences the onset of buckling. We can qualitatively reproduce this trend by considering the buckling ratio at 90% bound guest (Figure S2b).

However at relatively high CB[8] concentrations (CB[8]:stilbene = 10:1) the equilibrium shifts towards bound guests to the extent that the equilibrium dynamics are not a limiting factor and the buckling diameter saturates (Figure 2b). We reproduce the trend observed for the homoternary stilbene-stilbene cross-linking with strongly binding MV^{2+}-stilbene cross-linking ($K_a \sim 10^9$ M^{-2}), which confirms that equilibrium dynamics are not fundamental to the onset of buckling in the high CB[8] concentration regime considered here (Figure 2a and Figure S1).

Kinetic experiments

Two time scales were adjusted to assess if the kinetics play a role in the capsule formation process. These time scales were the amount of time before the start of the evaporation (droplet ageing) and the evaporation rate. For droplet ageing, the microdroplet emulsion was collected from the microfluidic device and then stored in a sealed glass vial. Portions of this emulsion were then taken at different time points and evaporated on a glass slide. Separately, the rate of evaporation was varied using a heated microscope stage (Linkham PE94) during drying on the glass substrate.

Table S1. Summary of kinetic studies of (PVA-mv·PVA-stil)⊂CB[8] capsule formation with different droplet storage times and different evaporation rates. Changing these time scales does not appear to have an influence the buckling ratio $\frac{R_{buck}}{R_0}$.

Sample	Storage time (min)	Evap. Time (min)	D_0 / μm (st. dev.)	D_{buck} / μm (st. dev.)	$\frac{R_{buck}}{R_0}$
0 h, 60 °C	0	5-7	58 (2)	19.4 (0.8)	0.34 (0.02)
0 h, RT	0	32-36	59 (1)	19.1 (0.6)	0.32 (0.02)
1 h, RT	60	12-14	61 (2)	18.4 (0.8)	0.30 (0.01)
4 h, RT	240	12-14	60 (1)	17.9 (0.8)	0.30 (0.01)

The results of these procedures are shown in Table S1. Neither ageing the droplet before evaporation or increasing the evaporation rate resulted in a significant change in the buckling diameter. However, the samples that were stored before evaporation required much less time to reach the buckling transition. This may be a result of different amounts of oil between the control sample taken directly from the microfluidic outlet, and the stored sample pipetted onto the glass slide.

Despite the substantially shorter evaporation time with the heated sample (Table S1: "0 h, 60 °C") within error the results match the control experiment ("0 h, RT"). Heating the sample during the evaporative step could have at least two effects on the kinetics. Firstly, the evaporation rate is increased and so the amount of time before capsule buckling is decreased. Secondly, chemical reactions, including supramolecular complexation, usually occur at increased rates at higher temperatures. In principle it is possible that two or more competing thermal effects could cancel each other out, however in practice this would be an unlikely coincidence.

In summary, there appears to be no significant kinetic influence on the buckling transition over the conditions and time scale ranges assessed here.

Thickness to radius ratio, T/R

The "double-wall" thicknesses of collapsed microcapsules dried onto glass slides were measured by optical interferometry[1,3] and tapping mode atomic force microscopy (Keysight 5500 SPM, Bruker TAP150A cantilevers).

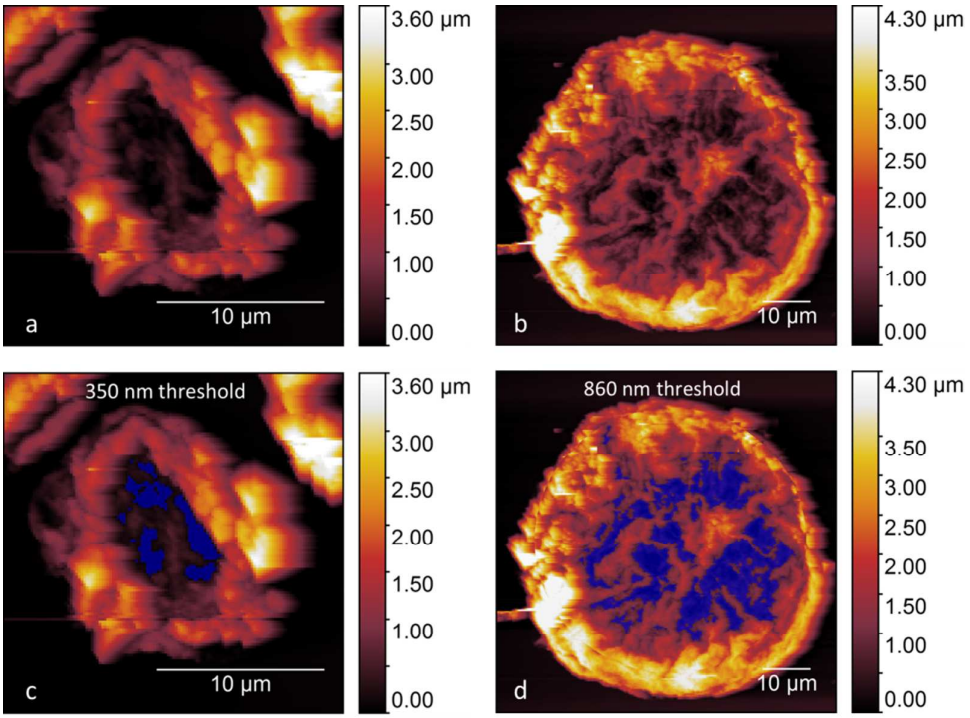

Figure S3. AFM images of dried (PVA-stil·PVA-mv)⊂CB[8] microcapsules with buckling diameters of (a) 23 ± 1 µm and (b) 74 ± 4 µm. For (b) the initial droplets were larger giving more polymeric material and so larger capsules. The images are leveled and offset such that the substrate surface is at 0. Corresponding thresholded images are shown in (c) and (d). The thresholded areas (blue) are of lower thickness than the labeled values. The areas surrounding the capsules are excluded from the thresholds for clarity. Overall a larger capsule buckling radius is found to correspond to a greater wall thickness, consistent with a constant ratio $\left(\frac{T}{R}\right)_{buck}$.

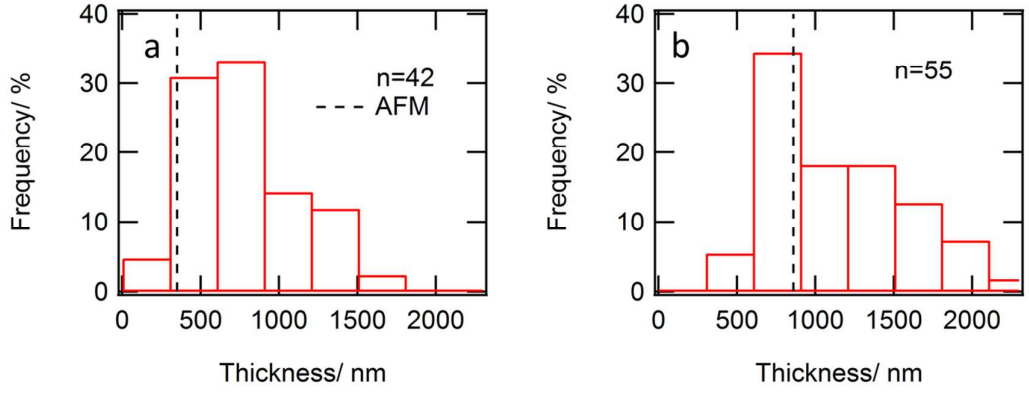

Figure S4. Interferometric "double-wall" thickness histograms for (PVA-stil·PVA-mv)⊂CB[8] microcapsules with buckling diameters of (a) 23 ± 1 µm and (b) 74 ± 4 µm, as in Fig. S3. The associated double-wall thicknesses as determined by AFM are inidicated by the dashed line. The "true" double-wall thicknesses correspond to the lower end of the measured distributions, while the higher end of the distributions are a result of capsule crumpling.

Confocal imaging

It is necessary that the majority of polymer assembles at the interface in order for the thickness measurements of collapsed shells to be representative of shell wall thickness. Otherwise residual material would contribute to the measured thickness.

Using fluorescently labelled polymer and confocal cross-sectioning it is found that practically all of the material assembles at the droplet interface (Figure S5).

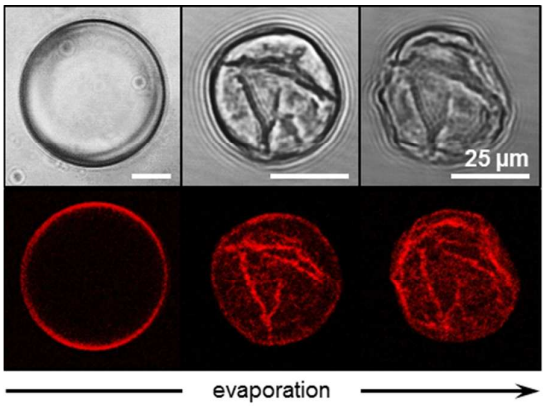

Figure S5. Transmission (top) and laser scanning confocal micrographs (LSCM, bottom) of the evaporation driven transition from microdroplets to microcapsules for aqueous droplets containing (PVA-mv·PVA-stil)⊂CB[8] pre-accumulated at the oil/water interface.

References

(1) Parker, R. M.; Zhang, J.; Zheng, Y.; Coulston, R. J.; Smith, C. A.; Salmon, A. R.; Yu, Z.; Scherman, O. A.; Abell, C. Electrostatically-Directed Self-Assembly of Ultra-Thin Supramolecular Polymer Microcapsules. *Adv. Funct. Mater.* **2015**, *25* (26), 4091–4100.

(2) Grasberger, B.; Minton, A. P.; DeLisi, C.; Metzger, H. Interaction between Proteins Localized in Membranes. *Proc. Natl. Acad. Sci. U. S. A.* **1986**, *83* (17), 6258–6262.

(3) Salmon, A. R.; Capener, M. J.; Baumberg, J. J.; Elliott, S. R. Rapid Microcantilever-Thickness Determination by Optical Interferometry. *Meas. Sci. Technol.* **2014**, *25* (1), 015202.